

ScienceDirect

Procedia CIRP 121 (2024) 67-72



11th CIRP Global Web Conference (CIRPe 2023)

Thermal redistribution of compressive residual stress introduced by interlayer laser shock peening in hybrid additive manufacturing

George H. Klein^a, Rakeshkumar Karunakaran^b, Michael P. Sealy^{b*}

^aMechanical and Materials Engineering Department, University of Nebraska-Lincoln, NE 68508, U.S.A. ^bSchool of Mechanical Engineering, Purdue University, IN 47906, U.S.A.

* Corresponding author. Tel.: +1-765-496-7569; E-mail address: msealy@purdue.edu

Abstract

The objective of this research was to quantify the change in magnitude and depth of compressive residual stress (CRS) retained in the subsurface by interlayer coldworking when subjected to localized annealing that superimposed tensile stress. The approach was to hybridize additive manufacturing of AlSi10Mg alloy by coupling powder bed fusion (PBF) with laser shock peening (LSP) and characterize the resultant residual stress state by the hole-drilling method. The research found localized annealing from layer deposition formed two distinct regions in the subsurface, which was driven by localized and bulk stress redistribution. The experiments also showed that residual stress redistribution from LSP reached 550 μ m into the subsurface, whereas local annealing from the deposition of layers extended only to a depth of 160 μ m. Hence, compressive stress imparted by LSP was not entirely canceled by local annealing from PBF. This work provides the first quantification of the stress state response of hybrid additively manufactured parts to thermal loads and is fundamental to improving part performance through increased functional reliability, fatigue life, and corrosion resistance.

© 2023 The Authors. Published by Elsevier B.V.
This is an open access article under the CC BY-NC-ND license (https://creativecommons.org/licenses/by-nc-nd/4.0)
Peer-review under responsibility of the scientific committee of the 11th CIRP Global Web Conference

Keywords: Thermal cancellation, residual stress, hybrid additive manufacturing

1. Hybrid additive manufacturing

1.1. Interlayer surface treatments in hybrid additive manufacturing

Hybrid additive manufacturing refers to a cyclic process chain constituting additive manufacturing with one or more secondary processes or energy sources to alter part quality and functionality [1]. The secondary process is utilized throughout the build process, either intermittently or continuously, to functional changes to manufactured components. The secondary processes affect bulk functionality by locally altering material behavior using interlayer surface treatments, such as ultrasonic peening [2] and laser shock peening [3]. The surface treatments performed on intermittent

throughout a build relax the adverse residual tensile stresses that build up during AM. Mitigating tensile residual stress along with other improvements in material properties like grain refinement and microhardness enhances fatigue life [4] and corrosion kinetics [5] of manufactured parts.

1.2. Laser shock peening as an interlayer surface treatment for hybrid additive manufacturing

Laser shock peening (LSP) is a high strain rate mechanical process that introduces large compressive residual stress in the subsurface that extends beyond 1 mm into the bulk material [6]. This capability to impart deep compressive residual stress makes LSP a suitable secondary process in hybrid AM to alter local stress fields and, thus, the bulk behavior. Fig. 1

presents a schematic of the hybrid AM process chain, wherein LSP was performed on the intermittent surfaces of layers deposited by AM.

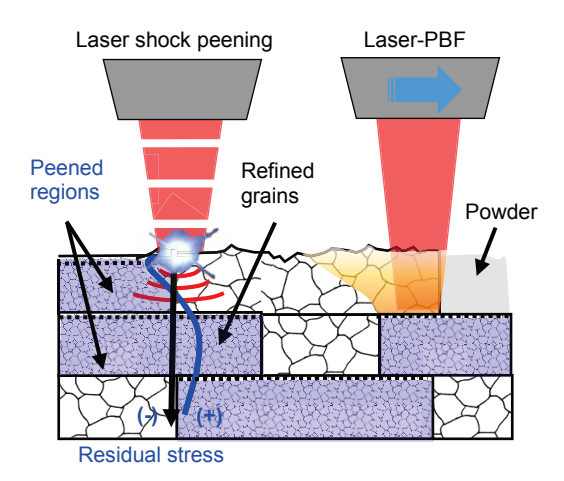


Fig. 1 Schematic of hybrid AM using interlayer laser shock peening during laser powder bed fusion.

Early computational investigations on the implementation of interlayer LSP during AM suggested that CRS imparted by LSP were not completely erased (i.e., annealed) by the thermal loads from the deposition of subsequent layers. Recent experimental investigations substantiated the presence of interlayer residual stress and grain refinement that favorably improved bulk mechanical and chemical behavior [7, 8].

1.3. Knowledge gap in understanding thermal redistribution of residual stress in hybrid AM

The current state of research in hybrid AM presents limited experimental evidence on how compressive residual stress over a mechanically treated surface redistribute when hot layers are deposited by AM. That is, investigations did not quantify what specific changes occur to the residual stress state of hybrid AM parts when layers are printed over an LSP-treated surface. This interaction of compressive residual stress in the subsurface with tensile stress from the deposition of new layers is referred to as thermal redistribution. This phenomenon must be understood to optimize the placement of interlayer LSP during AM. Therefore, the objective of this research was to quantify thermal redistribution in a compressively stressed subsurface when subjected to localized heat from the deposition of layers.

2. Experiment to characterize thermal redistribution of residual stress in hybrid AM

2.1. Sample fabrication

Five unique sample groups were produced for this experiment, defined as A-E. A complete description of the sample groups is provided in Table 1. All five groups were manufactured using a Matsuura Lumex Avance-25 reactive PBF machine with processing parameters outlined in Table 2. All samples in this experiment were printed using the popular aluminum alloy AlSi10Mg. Each sample group consisted of triplicates of 20 mm x 20 mm x 10 mm rectangular samples with 200 layers printed on a 12.5 mm baseplate.

Sample groups A-D were subjected to identical LSP treatments as per the process parameters mentioned in Table 3. Sample surfaces were peened at 200% coverage (*i.e.*, two rounds of peening) with 50% overlap between adjacent peened spots. Black tape and water were used as the ablative layer and confining medium, respectively. Two, four, and six additional layers were printed over sample groups B, C, and D, respectively, to thermally redistribute compressive stress imparted by LSP. The fabricated samples are shown in Fig. 2.

Table 1 Thermal cancellation sample groups

Group	LSP	Additional	
Огоир	treatment	layers	
Surface peened (A)	Yes	0	
2 Layer hybrid (B)	Yes	2	
4 Layer hybrid (C)	Yes	4	
6 Layer hybrid (D)	Yes	6	
As built (E)	No	0	

Table 2 AM process parameters

Sintering parameter	Value		
Laser power	360 W		
Spot diameter	300 µm		
Scanning speed	600 mm/s		
Hatching pitch	0.27 mm		
Layer thickness	50 µm		

Table 3 LSP process parameters

Sintering parameter	Value		
Laser pulse energy	1.27 J		
Laser spot size	2 mm		
Laser intensity	5.05 GW/cm ²		
Coverage	200%		
Overlap	50%		

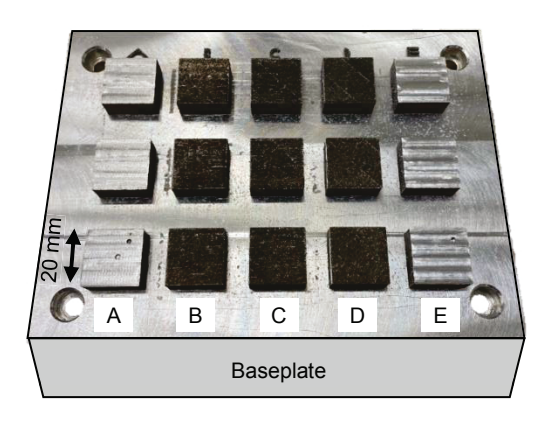


Fig. 2 Samples fabricated to characterize thermal redistribution of residual stress.

2.2. Characterization of residual stress by the hole-drilling method

The hole drilling method was selected for residual stress measurement because of its ability to accurately capture the residual stress state of samples up to a depth of 1 mm. The MTS 3000-Restan hole drilling system (SINT Technology, Italy, Fig. 3a) was used to characterize the residual stress state of the printed samples. Residual stress was calculated as per ASTM E837-13 [9], which defines the standard procedure for extended non-uniform residual stress calculation from strain measurements captured during hole drilling. Each hole was drilled to a depth of 1.5 mm in increments of 0.016 mm for a total of 94 steps. This resulted in a complete description of residual stress as a function of depth.

Strain gauges (Fig. 3b) adhered to samples before hole-drilling required a smooth top surface (Fig. 3c,d). To achieve this, the samples were separated by cutting the baseplate with a bandsaw. The sample groups B-D were hand-polished using 600-grit sandpaper and water. Sample heights were monitored to allow for accurate curve shifts during the analysis phase.

3. Analysis of residual stress profile after hole-drilling to quantify thermal redistribution

3.1. Experimental characterization of thermal redistribution limit

Fifteen data sets were obtained from hole-drilling of the printed sample groups A-E. Each data set described the residual stress state of its corresponding sample group as a function of depth from the surface. The datasets for the sample groups consisted of maximum and minimum principal stress as a function of depth, which was averaged at each depth location to calculate the middle principal stress. The zero point

along the depth axis was defined at the top surface of group A samples, *i.e.*, the sample with surface peening. As layer addition in sample groups B-D increased sample height, the middle principal stress curves were offset to ensure consistency along the depth axis. The residual stress curves of sample groups B, C, and D were shifted by $20~\mu m$, $100~\mu m$, and $170~\mu m$ to the left of the group A curve. This shift was comparable to their theoretical values of $0~\mu m$, $50~\mu m$, and $100~\mu m$. the theoretical shifts were calculated by height increments of $100~\mu m$ attained by adding two $50~\mu m$ tall layers across sample groups. The differences between theoretical and experimental shifts may be from the calibration of print bed height after LSP.

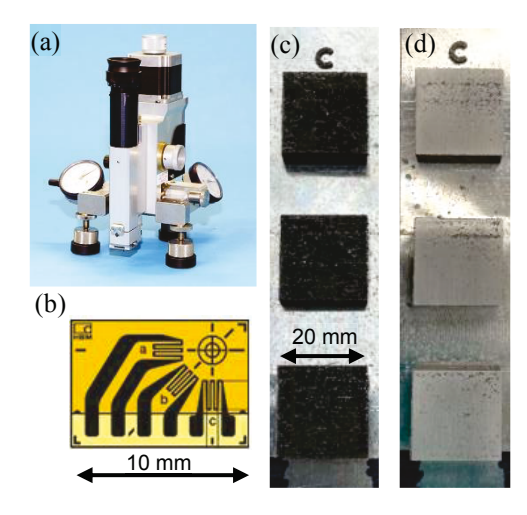


Fig. 3 (a) Hole drilling setup; (b) strain gauge; and representative sample surfaces from groups B-D (c) before and (d) after polishing.

Fig. 4 shows that LSP treatments had a substantial impact on the resultant residual stress state of sample groups A-D. Tensile residual stress developed in the as-printed sample (sample E) was mitigated across all four LSP groups (A-D) to a depth of at least 1 mm. This result showed that the deposition of layers did not thermally anneal compressive stress incorporated by interlayer LSP treatments. Instead, the compressive residual stress was thermally redistributed near the interface where additional layers were deposited. The samples showed an inflection point at 0.1 mm depth moved towards the surface with added layers. This movement was seen regardless of high standard deviation near the top surface of the samples. All replicates within sample groups exhibited similar translations of the inflection point.

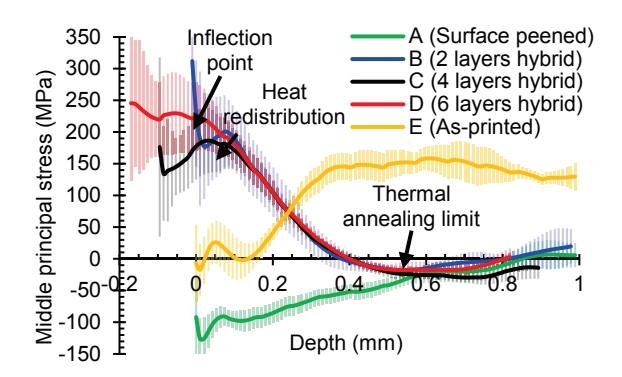


Fig. 4 Residual stress measured as a function of depth in the sample groups A-E.

Thermal redistribution is the restructuring of the residual stress state of hybrid AM parts due to excess thermal loads derived from the deposition of additional layers. Graphically, this phenomenon was presented in this research as the difference between the residual stress curves of the surface peened samples (group A) and the hybrid AM samples (groups B-D). The limit of thermal redistribution was identified 160 µm deep below the LSP treated interfaces, where the stress states of sample groups B-D merged.

3.2. Modeling the thermal redistribution limit

Thermal redistribution of residual stress within metals will cease to occur when the temperature of the material drops below 50% of its recrystallization temperature, *i.e.*, below the recovery temperature. Since AlSi10Mg recrystallizes at 853 K, the expected recovery temperature was 427 K [10]. By assuming the meltpool to be 71 μ m deep [10], the depth of thermal redistribution was calculated using Newton's law of cooling, as stated in Eqn. 1.

$$Q = \frac{k A \Delta T}{\Delta x}$$
 Eqn. 1

In this equation, Q is the laser heat during AM, A is the cross-section of the laser spot, k is the thermal conductivity, ΔT is the difference between the recrystallization and recovery temperatures, and Δx is the limit of thermal redistribution. A complication with this simplified model is that thermal conductivity of AlSi10Mg is highly dependent on temperature [10]. The rate of heat absorption is also nonuniform and highly dependent on layer height and powder geometry. Therefore, assumptions were made in this modeling approach to maintain simplicity while estimating the limit of thermal redistribution. A lower estimate of 100 μ m was calculated assuming thermal conductivity as 175 W/mK, laser heat input as 360 W

with a 50% absorption coefficient, and with the laser spot area as 7.07E-2 mm². An upper estimate of $145\mu m$ was calculated by assuming a thermal conductivity of 175 W/mK, heat input of 360 W with a 20% absorption coefficient, and a laser spot area of 7.07×10^{-2} mm². These estimates were based on a range of thermal absorptivity cited in literature, as thermal absorptivity of the powder bed is difficult to calculate owing to powder particle shape and size distribution. Based on the estimated values, the thermal redistribution limit was calculated as $100-145 \mu m$ from the free surface of the layer being deposited. This calculated range for the limit of thermal redistribution was close to the experimentally determined depth of $160 \mu m$ (Fig. 4).

Prior to this depth, it is believed that the temperature of the material was above 427 K, evidenced by the unique behavior of each sample group. Within this region, addition of new layers affected the residual stress state. Specifically, by increasing the number of additional layers deposited on top of the peened layer, the magnitude of stress oscillation is reduced. The 2-layer hybrid set oscillated faster and to a higher state of residual stress than the 4- and 6-layer hybrid sets. This was explained by the fundamental requirement of force equilibrium. The 2-layer hybrid set has much less material through which it can offset the compressive stresses imparted onto the peened layer, thus, the stresses oscillated aggressively.

3.3. Thermal annealing limit

While printing on a peened surface introduced tensile residual stress in upper layers, the stress state in the four hybrid AM curves became similar after 0.55 mm (Fig. 4). This depth was determined as the limit of thermal annealing, as the stress below this depth was indifferent regardless of the number of additional layers deposited over the peened surface. That is, the thermal annealing limit represents the depth below which addition of new layers caused limited change in residual stress. The part retained the compressive residual stress imparted by LSP below this depth despite the addition of several layers by AM.

3.2. Modeling residual stress behavior

The residual stress data in Fig. 4 shows two distinct regions in the hybrid AM parts (sample groups B-D). The first region spans from the free surface of the samples to the "heat redistribution limit," which is at a depth of 160 µm beyond the peened layer. The residual stress in this region was highly sensitive to the number of added layers. In this first region, the residual stress oscillated for the 2- and 4-layer hybrid groups (*i.e.*, sample groups B and C, respectively) and

stabilized for the 6-layer hybrid group (*i.e.*, D). This portion of the residual stress was represented by a sinusoid whose amplitude depended on the number of additional layers deposited. The oscillation period of the sinusoid increased as per the distance of the free surface from the heat redistribution limit. This sinusoid adequately described the residual stress ($\sigma_{r,1}$) in the region between the heat distribution limit and the free surface, and is provided in Eqn. 2. In this equation, L is the number of added layers, d is the distance between the heat redistribution limit and the free surface, γ is a 1.33X amplification of the as-built tensile residual stress, and α is a scaling factor.

$$\sigma_{r,1} = -\frac{\alpha}{L} sin\left(\frac{2\pi}{d}x\right) + \gamma$$
 Eqn. 2

The second region of residual stress behavior, beginning at the heat redistribution limit and extending to the final depth of 1 mm, is consistent across all three hybrid groups. The curves began at the as-built tensile residual stress of the bulk, characterized by the right side of the "as-built" curve in Fig. 4, and decay to a state of neutral stress. The second region's residual stress, $\sigma_{r,2}$, was described by an exponential decay function, Eqn. 3, with β as the as-built tensile residual stress, ω as a decay factor, and δ as a shift factor.

$$\sigma_{r,2} = (\beta + \delta)(1 - \omega)^x - \delta$$
 Eqn. 3

These residual stress models were used to generate prediction curves for each of the 2-, 4-, and 6-layer hybrid samples corresponding to group labels B-D, as shown in Fig. 5. Parameter values for each model were attained by manual curve fitting and are shown in Table 4. The α and ω parameters were selected based on curve fitting for the experimental data. The α value was equivalent to β value for the 2- and 4-layer hybrid sets, and only differed in sign for the 6-layer hybrid set.

The average error was calculated as the difference between the residual stress measurements from the three replicates with respect to the model along the entire 1mm depth. Compared to the experimental data, the average error of the $\sigma_{r,1}$ models for the 2-, 4- and 6-layer hybrid groups were 39.2%, 24.9%, and 13.6%, respectively. The average error of the $\sigma_{r,2}$ models for the 2-, 4- and 6-layer hybrid groups were 30.7%, 15.3%, and 26.9%, respectively. The $\sigma_{r,2}$ error averages were trimmed, meaning any error values greater than 100% were removed from the total average, as the untrimmed average error ranged from 20-200%. Trimming reduced the influence of the tail regions of the residual stress curves, which diverge

quickly from the model curves. The divergence is likely driven by strain measurement error, as the accuracy of the residual stress drill near its maximum depth is low. This trimming had little effect on the confidence of the $\sigma_{r,2}$ model's error assessment. The model curves are plotted over the experimental curves in Fig. 5. The discontinuity between the two behavior regions exists because stress field interactions were ignored within the two models.

Table 4 Residual stress model parameters

Sample group	L	d (μm)	α	γ (MPa)	β (MPa)	ω	δ (MPa)
В	2	181	150	200	150	0.01	15
С	4	266	150	200	150	0.008	30
D	6	341	-150	200	150	0.007	30

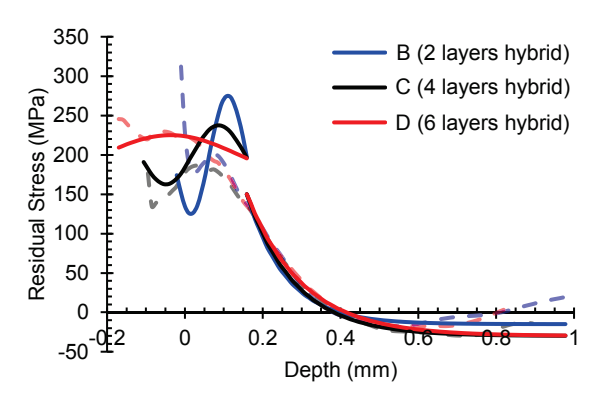


Fig. 5 Fitted model for modeling thermal redistribution of residual stress. (Solid and dashed lines represent fitted model and experimental data, respectively.)

4. Summary and conclusions

In this research, hybrid AM using LSP was performed to quantify the magnitude and depth of compressive residual stress lost due to thermal loading derived from the deposition of additional layers. The following statements summarize the knowledge gained from this research:

- Deposition of layers over LSP-treated surfaces alters residual stress up to a depth termed as the thermal annealing limit. The thermal annealing limited was determined as 0.55 mm for AlSi10Mg printed with an energy density of 44 J/mm³.
- Deposition of layers over LSP-treated surfaces affects residual stress state to a depth termed as the heat redistribution limit. This depth was

- determined as 160 µm beyond the peened surface for AlSi10Mg printed for this research.
- The residual stress behavior of hybrid AM parts within the heat redistribution zone was oscillatory. The magnitude of oscillations damped with the number of added layers.
- 4. The residual stress behavior of hybrid AM parts beyond the heat redistribution limit decayed exponentially.
- A model was proposed that reasonably captures key features pertaining to heat from material deposition in hybrid AM.

The ideas of thermal cancellation and the limit of heat dependent stress redistribution provide a comprehensive understanding how the modified residual stress states of hybrid AM parts respond to additional layer deposition. They showed that the residual stress state of a material is affected by excess thermal loads well beyond the depth at which the material cools below its recovery temperature.

In the future, a new hybrid AM experiment using the same process parameters from this research will be performed, where LSP will is performed every 11 layers (*i.e.*, 0.55 mm). This experiment would test the outcome of this research, which is that intermittent LSP performed at a distance equivalent to the limit of thermal cancellation would neutralize the residual stress within hybrid AM parts.

Acknowledgments

This research was supported in part by NSF CAREER Award 1846478 and performed in part in the Nebraska Nanoscale Facility (NSF ECCS: 1542182) and NEAT Lab supported by the Nebraska Research Initiative.

References

- [1] Sealy, M.P., Madireddy, G., Williams, R.E., Rao, P., Toursangsaraki, M., 2018. Hybrid processes in additive manufacturing, Journal of manufacturing science and engineering 140.
- [2] Gale, J., Achuhan, A., 2017. Application of ultrasonic peening during DMLS production of 316L stainless steel and its effect on material behavior, Rapid Prototyping Journal 23, p. 1185-1194.
- [3] Lu, H., Deng, W., Luo, K., Chen, Y., Wang, J., Lu, J., 2023. Tailoring microstructure of additively manufactured Ti6Al4V titanium alloy using hybrid additive manufacturing technology, Additive Manufacturing 63, p. 103416.
- [4] Kalentics, N., de Seijas, Manuel Ortega Varela, Griffiths, S., Leinenbach, C., Logé, R.E., 2020.

- 3D laser shock peening A new method for improving fatigue properties of selective laser melted parts, Additive Manufacturing 33, p. 101112.
- [5] Sealy, M.P., Karunakaran, R., Ortgies, S., Madireddy, G., Malshe, A.P., Rajurkar, K.P., 2021. Reducing corrosion of additive manufactured magnesium alloys by interlayer ultrasonic peening, CIRP Annals.
- [6] Gujba, A.K., Medraj, M., 2014. Laser peening process and its impact on materials properties in comparison with shot peening and ultrasonic impact peening, Materials 7, p. 7925-7974.
- [7] Lu, J., Lu, H., Xu, X., Yao, J., Cai, J., Luo, K., 2020. High-performance integrated additive manufacturing with laser shock peening –induced microstructural evolution and improvement in mechanical properties of Ti6Al4V alloy components, International Journal of Machine Tools and Manufacture 148, p. 103475.
- [8] Kalentics, N., Boillat, E., Peyre, P., Gorny, C., Kenel, C., Leinenbach, C., Jhabvala, J., Logé, R.E., 2017. 3D laser shock peening – a new method for the 3D control of residual stresses in selective laser melting, Materials & Design 130, p. 350-356.
- [9] ASTM, 2021. Standard Test Method for Determining Residual Stresses by the Hole-Drilling Strain-Gage Method.
- [10] Cai, L., Liang, S.Y., 2021. Analytical Modelling of Temperature Distribution in SLM Process with Consideration of Scan Strategy Difference between Layers, Materials 14, p. 1869.